Incorporating Surface Emissivity into a Thermal Atmospheric Correction

Nathaniel A. Brunsell and Robert R. Gillies

Abstract

The issue of incorporating surface emissivity into a thermal atmospheric correction of thermal remotely sensed data is addressed. The Normalized Difference Vegetation Index (NDVI) is derived using atmospherically corrected surface reflectance values, which is subsequently used to estimate the percent of vegetation cover. Surface emissivity is approximated by a linear interpolation between a minimum bare soil emissivity and a maximum vegetation value of emissivity. An application of the method to an image over the Southern Great Plains 1997 (SGP97) Hydrology Experiment for the Advanced Very High Resolution Radiometer (AVHRR) band 4 demonstrates temperature corrections up to 8°C, with a mean correction of 3.7°C. The temperatures within the fully vegetated pixels show good agreement with air temperature measurements at the time of satellite overpass.

Introduction

A primary limitation for the practical application of thermal remote sensing (i.e., in the 8- to 14-μm region of the electromagnetic spectrum) is the necessity of determining accurate radiometric temperatures (i.e., temperature measured by a radiometer after emissivity has been taken into account) at the surface, which requires knowing the pixel-scale surface emissivity. This issue has attracted significant attention over the past several years, and as yet a practical methodology has eluded researchers (for recent reviews of methodologies and the associated errors, see Sobrino *et al.* (2001) and Qin and Karnieli (1999)). Many researchers have chosen to simply ignore the issue altogether, or to assign a constant value of emissivity to all pixels in the dataset. However, this neglects the inherent heterogeneity of the surface, and this is what is of most interest when analyzing remotely sensed data.

Any methodology for estimating emissivity is certainly better than an assumption that every surface is a perfect emitter. Natural surfaces are not perfect emitters, and therefore have an emissivity value less than one. Therefore, any correction that reduces the emissivity to a more realistic value is reducing the error when compared to a default emissivity value set to one.

There is sufficient reason to believe that the pixel-scale emissivity of a surface will be related to the amount of vegetation that is present (van de Griend and Owe, 1993), due to the relatively high values of emissivity of vegetation compared to that of other natural surfaces. This general method for incorporating emissivity as a function of the atmospherically corrected red and near-infrared bands is referred to, by Sobrino *et al.* (2001), as NDVI threshold methods.

Previous research has focused on the incorporation of emissivity assuming an atmospheric correction has already been performed. However, the literature is lacking in a clear description of a methodology on how to perform an atmospheric correction in the thermal portion of the spectrum for satellite remote sensing with emissivity incorporated as part of the algorithm. Accurate determination of radiometric surface temperatures requires information concerning the state of the atmosphere at the time of satellite overpass.

An alternate method that is widely applied for atmospheric corrections of temperature is the split window (e.g., McMillan (1975) and Walton *et al.* (1990)). This method has the benefit of not requiring prior knowledge of atmospheric conditions (Sobrino *et al.*, 1994) as the transmittance effects are estimated as a function of brightness temperatures in band 5 and band 4 based on many assumptions. However, split window formulations for radiant temperatures require empirically determined coefficients based on the type of surface under investigation. Given the heterogeneity that exists at the 1-km scale of the AVHRR sensor, the derivation of so many empirical coefficients is unrealistic in terms of a practical methodology. In addition, split window methods have errors on the order of 2 K (Kant and Badarinath, 2000; Casseles *et al.*, 1997) over land surfaces. These errors are largely attributable to the atmospheric conditions at the time of overpass because the method relies on the assumption that atmospheric temperatures are fairly close to surface temperatures (Ouaidrari *et al.*, 2002). These methods were developed for the estimation of sea surface temperatures (where the above assumption holds), and although these methods are commonly applied to land surfaces, they are not necessarily the most appropriate.

The use of a radiative transfer model such as Modtran and a local radiosonde profile permits the accurate determination of surface temperatures on an image-by-image basis. Both radiative transfer models and split window techniques assume a spatially homogeneous atmosphere at the time of satellite overpass (Sobrino *et al.*, 1994); however, the radiative transfer method is initialized with a detailed sounding of the atmospheric conditions (particularly water vapor).

In this study, the thermal correction algorithm briefly described in Brunsell and Gillies (2001) is developed in more detail. This method accounts for both atmospheric emission and surface emissivity effects. The emissivity is determined by linearly relating the fractional vegetation (Fr) developed by Gillies and Carlson (1995) and Gillies *et al.* (1997) to a bare soil

N.A. Brunsell is with the Department of Plants, Soils and Biometeorology, Utah State University, Logan, UT 84322-4820 (brunsell@cc.usu.edu).

R.R. Gillies is with the Department of Plants, Soils and Biometeorology, and the Department of Aquatic, Watershed and Earth Resources, Utah State University, Logan, UT 84322-4820 (rgillies@nr.usu.edu).

Photogrammetric Engineering & Remote Sensing
Vol. 68, No. 12, December 2002, pp. 1263–1269.

0099-1112/02/6812–1263$3.00/0

emissivity (Fr = 0.0) and a full vegetation emissivity (Fr = 1.0). The atmospheric calibration is obtained by multiple iterations of the radiative transfer model Modtran 3. The model is run for a range of scan angles and a multi-linear regression is set up, one that is easily applied for both an atmospheric correction as well as accounting for the effects of surface emissivity.

The method is applied to an AVHRR image from 02 July 1997 over the Southern Great Plains 1997 Hydrology Experiment site in Oklahoma. Specifically, the method is applied to band 4 of AVHRR although it could be applied to any other thermal remotely sensed data (e.g., Landsat TM, GOES). Band 4 was chosen over band 5 due to the presence of the atmospheric window in band 4 and the additional absorption issues involved with band 5.

Theoretical Background on Emissivity

Emissivity (ε, dimensionless) is defined as the ratio of emission of an actual surface to that of a perfect emitter at the same temperature as the object (T_{sfc}). The emission of any surface ($B_\lambda(T_{sfc})$) at a specified wavelength (λ) and temperature is given by the Planck equation: i.e.,

$$B_\lambda(T_{sfc}) = \frac{\varepsilon_\lambda C_1}{\lambda^5\left(\exp\left(\frac{C_2}{\lambda T_{sfc}}\right) - 1\right)} \quad (1)$$

where $C_1 = 1.19028 \times 10^{-16}\,\mathrm{W\,m^{-6}sr^{-1}}$, and $C_2 = 0.01438\,\mathrm{K\,m}$.

Depending on the actual surface temperature, emissivity can elicit an effect in the range of 1 to 5°C when translating brightness temperatures to radiometric surface temperatures. Due to temperature errors of this magnitude, any inference about surface processes which are dependent upon accurate temperature measurements, e.g., the determination of sensible and latent heat fluxes (*ref.*, French *et al.*, 2001) can be markedly different if emissivity is not taken into account.

The Relationship between Vegetation and Emissivity

There is a body of literature (e.g., van de Griend and Owe (1993), Olioso (1995), Valor and Caselles (1996), and Caselles *et al.* (1997)) that deals with the relationship between the amount of vegetation present within a pixel and the pixel's emissivity. Many of these studies focused on the normalized difference vegetation index (NDVI). NDVI is defined as a function of the surface derived reflectance in the red band $\rho 1$ and the near-infrared band $\rho 2$: i.e.,

$$\mathrm{NDVI} = \frac{\rho_2 - \rho_1}{\rho_2 + \rho_1}. \quad (2)$$

The surface reflectance values are derived from at-sensor reflectance using a regression obtained from the output of the radiative transfer model Modtran and a local radiosonde profile. It is important to use surface reflectance in Equation 2 due to the decrease in variance observed when using apparent (top of atmosphere) NDVI compared to surface values. This decrease in variance (and associated errors) will then be propagated through all later calculations.

Van de Griend and Owe (1993) described a logarithmic relationship between NDVI and emissivity. As pointed out by Olioso (1995), however, this relationship is only appropriate for regions similar to that used by van de Griend and Owe (1993) (i.e., a semi-arid region in Botswana).

Several studies have attempted to relate NDVI to percent vegetation cover (Valor and Caselles 1996). Casselles *et al.* (1997) used a scaled version of NDVI (which, following the terminology of Gillies *et al.* (1997) is referred to as N^*) to represent the percentage of vegetation present within a pixel: i.e.,

$$N^* = \frac{\mathrm{NDVI} - \mathrm{NDVI_0}}{\mathrm{NDVI_{max}} - \mathrm{NDVI_0}} \quad (3)$$

where $\mathrm{NDVI_0}$ is the NDVI value corresponding to bare soil, and $\mathrm{NDVI_{max}}$ is the value corresponding to full vegetation. Gillies *et al.* (1997) presented a relationship relating N^* to fractional vegetation cover ([0,1] dimensionless): i.e.,

$$Fr = N^{*2}. \quad (4)$$

Note that this is a nonlinear function due to the nonlinear relationship between NDVI and LAI (i.e., NDVI values saturate at higher LAI values).

Assuming an image is comprised of a two-component soil and vegetation system, the emitted radiance from the pixel is

$$\varepsilon_i\sigma\overline{T^4} = \varepsilon_v\sigma\overline{T_v^4} + \varepsilon_s\sigma\overline{T_s^4} \quad (5)$$

where ε_v represents the emissivity of the vegetation, ε_s is the emissivity of the soil, and ε_i is the pixel's emissivity. The effective emissivity of the pixel can be written as a function of the fractional vegetation cover as

$$\varepsilon_i = Fr \cdot \varepsilon_v + (1 - Fr) \cdot \varepsilon_s. \quad (6)$$

This is a reasonable extension due to the high emissivity of vegetated surfaces and the relatively lower emissivity of non-vegetated sites.

Atmospheric Correction of the Thermal Band

The radiance values received in the thermal region of the electromagnetic spectrum at a sensor carried onboard an orbiting satellite are classified into three categories. The first is the surface emission transmitted through the atmosphere (τL_{sfc}), the second is the atmospheric emission transmitted through the atmosphere above the point of emission ($L_\uparrow$), and the third is the atmospherically emitted downwelled radiance that is reflected by the surface and transmitted through the atmosphere ($\tau(1 - \varepsilon)L_\downarrow$). This can be formulated as

$$L_{sens} + \tau\lfloor L_{sfc} + (1 - \varepsilon)L_\downarrow\rfloor + L_\uparrow \quad (7)$$

where τ and ε are the transmissivity and atmospheric emission terms, respectively.

The atmospherically emitted surface reflected term is usually neglected (see the discussion in Sobrino *et al.* (1994); on the other hand, Schmugge *et al.* (1998) indicate an example where it is not neglected).

To calculate the transmissivity and atmospheric emission terms, the radiative transfer model Modtran 3 (Kniezys *et al.*, 1996) is used in conjunction with a local radiosonde profile. Modtran is iterated over the range of scan angles (θ) observed over the scene. Following surface emission, the atmospheric effects (transmission and emission) are primarily determined by the path length through the atmosphere, which can be approximated as a function of the scan angle of the sensor. The average transmissivity over the range of the thermal band calculated by Modtran is used in this correction. The upwelled atmospheric emission is calculated as the sum over the thermal band after the sensor response is taken into account (Kidwell, 1998).

The actual surface emission received at the sensor is determined by a modified form of the Planck equation which cascades the sensor response function. This is necessary due to the fact that the sensor does not record equally in every wavelength. The sensor response coefficients are multiplied by the Planck function at each wavelength over the band and an expected range of surface temperatures from 0 to 60°C. The

resulting radiance value is summed over the band that represents radiance as a function of surface temperature as the sensor would observe it. This effect is approximated by a separate second-order polynomial equation for each emissivity value (1.0 to 0.9). The form of the equation is

$$L_{sfc,\varepsilon} = a_0 + a_1 T_{sfc} + a_2 T_{sfc}^2 \quad (8)$$

where the a_i terms vary with the value of emissivity (see Table 1).

Incorporating the transmissivity and upwelled-atmospheric emission, L_{sens} is a straightforward calculation: i.e.,

$$L_{sens} = \tau L_{sfc,\varepsilon} + L_{\uparrow}. \quad (9)$$

Once the radiance at the sensor is calculated, a relationship similar to Equation 8 is derived to calculate the at-sensor temperature as a third-order function of radiance. This regression equation does not take into account the emissivity term because the sensor assumes that all received radiation is emitted from a perfect emitter. Using the Planck equation, the sensor response function and a spectral increment of 0.074 μm, radiance values are summed over the entire band of interest (in this case, band 4 of AVHRR, although the method holds for any thermal sensor). The regression calculates the band 4 at-sensor temperatures as a function of the at-sensor radiances after accounting for the spectral response curve with an r^2 value of 0.998: i.e.,

$$T_{sens} = -69.04 + 0.64 L_{sens} - 0.001 L_{sens}^2 + 1.01 \times 10^{-6} L_{sens}^3. \quad (10)$$

The final stage is to regress the range of modeled surface temperatures (0 to 60°C), at each scan angle (0 to 40°), and over the range of emissivities (0.94 to 1.0) to achieve a regression relationship valid for the atmospheric conditions at the time of satellite overpass: i.e.,

$$T_{sfc} = b_0 + b_1 \theta + b_2 \varepsilon + b_3 T_{sens}. \quad (11)$$

Downwelled Atmospheric Emission

One issue that can offset the temperature effects of emissivity is surface reflected downwelled atmospheric emission $(1 - \varepsilon)L_{\downarrow}$. As discussed previously, this term is often neglected. In order to justify the assumption that it can be neglected, a simple test was conducted.

In order to quantify the maximum effects that downwelled emission has on the determination of surface radiometric temperature, the Modtran calculated path emission was taken to equal the downwelled emission for a surface emissivity of 1.0. No transmission effects were taken into account between the atmospheric emission and the surface. Using emissivity values ranging from 0.9 to 0.98, the reflectivity of the surface to infrared radiation was assumed to equal one minus the emissivity (i.e., no transmission). Atmospheric transmission was taken into account for the path from the surface to the sensor. The sensor response was also taken into account. This test represents an overestimation of at-sensor radiance because one is neglecting transmissivity effects between the point of atmospheric emission and the surface (see Schott, 1997).

The effects of reflected thermal radiation were estimated by applying the Stefan-Boltzmann law with and without the addition of the surface reflected term. Using the Stefan-Boltzmann law represents the maximum effect, because it is the integrated radiance over the 3- to 30-μm region (this is considerably more radiance than band 4 of the AVHRR sensor). The maximum effect computed was a 1.8 percent difference in at-sensor radiance, which translates to a 1 percent change in surface radiometric temperature; this equates to an approximate 0.9°C for the atmospheric conditions (temperature and humidity profiles) present at the time of overpass. The true effect in band 4 AVHRR will be considerable less and is therefore neglected. Although this analysis demonstrated that the surface reflected atmospherically emitted radiation could be ignored for this case, it is important to note that this may not hold for all atmospheric conditions. Had the air temperature been warmer and more humid, this effect would have been more significant and would have to be taken into account.

TABLE 1. REGRESSION COEFFICIENTS FOR SURFACE RADIANCE AS A SECOND-ORDER FUNCTION OF TEMPERATURE (EQUATION 8)

Emissivity	a_0	a_1	a_2
1.0	134.72	2.43	0.014
9.8	132.02	2.39	0.013
9.6	129.33	2.34	0.013
9.4	126.63	2.29	0.013
9.2	123.94	2.24	0.012
9.0	121.24	2.19	0.012

Application to Southern Great Plains 1997

The described procedure was used to calculate the radiometric surface temperature for an Advanced Very High-Resolution Radiometer (AVHRR) image over the Southern Great Plains 1997 (SGP97) Hydrology Experiment measured on the afternoon of 02 July 1997. SGP97 was an interdisciplinary project to investigate spatial variation in soil moisture over much of the state of Oklahoma. The AVHRR image was georeferenced to the Universal Transverse Mercator (UTM) coordinate system, zone 14N, WGS1980 spheroid, NAD83 datum. The image subset for the analysis defined a square area of 512 by 512 pixels, with a pixel resolution of 1.1 km^2. The near-surface atmospheric conditions at the time of overpass consisted of an air temperature of 33°C and a dew point temperature of 21°C.

Running the radiative transfer model Modtran 3 and applying local radiosonde data, the AVHRR image was atmospherically corrected in the visible and near-infrared bands. The resulting surface reflectance values were used to calculate the fractional vegetation as outlined in Equations 2 to 4. The emissivity was computed using Equation 6 with a soil emissivity of 0.955 and a vegetation emissivity of 0.98, which are appropriate values for AVHRR band 4 (Schmugge, personal communication).

An important exception to the linear assignment of emissivity is those pixels that are covered by water bodies. Water has very low fractional vegetation, yet it has a high emissivity. In the practical application of this method, pixels covered by water were assigned an emissivity of 0.998. The water pixels were determined as pixels with an NDVI value less than 0.2. This value was chosen by personal inspection of the data and choosing a threshold value between known water bodies and non-water pixels within the image. Figure 1 presents the image of the emissivity values calculated using this method.

Using the methodology described, an atmospheric correction was conducted. The model was iterated with scan angles from 0 to 40° (in five-degree increments), and emissivity ranged from 0.84 to 1.00 (in increments of 0.02). Modtran was iterated over band 4 of the AVHRR at a spectral increment of 0.074 μm. The modeled radiometric surface temperature ranged from 0 to 60°C (increments of 10°C). The regression values for the final equation (Equation 11) were determined as $b_0 = 132.13$, $b_1 = -1.08 \times 10^{-4}$, $b_2 = -138.40$, and $b_3 = 1.17$. The r^2 value for this regression was 0.977. These coefficients are, of course, only applicable to the atmospheric conditions that were present at the time of satellite overpass.

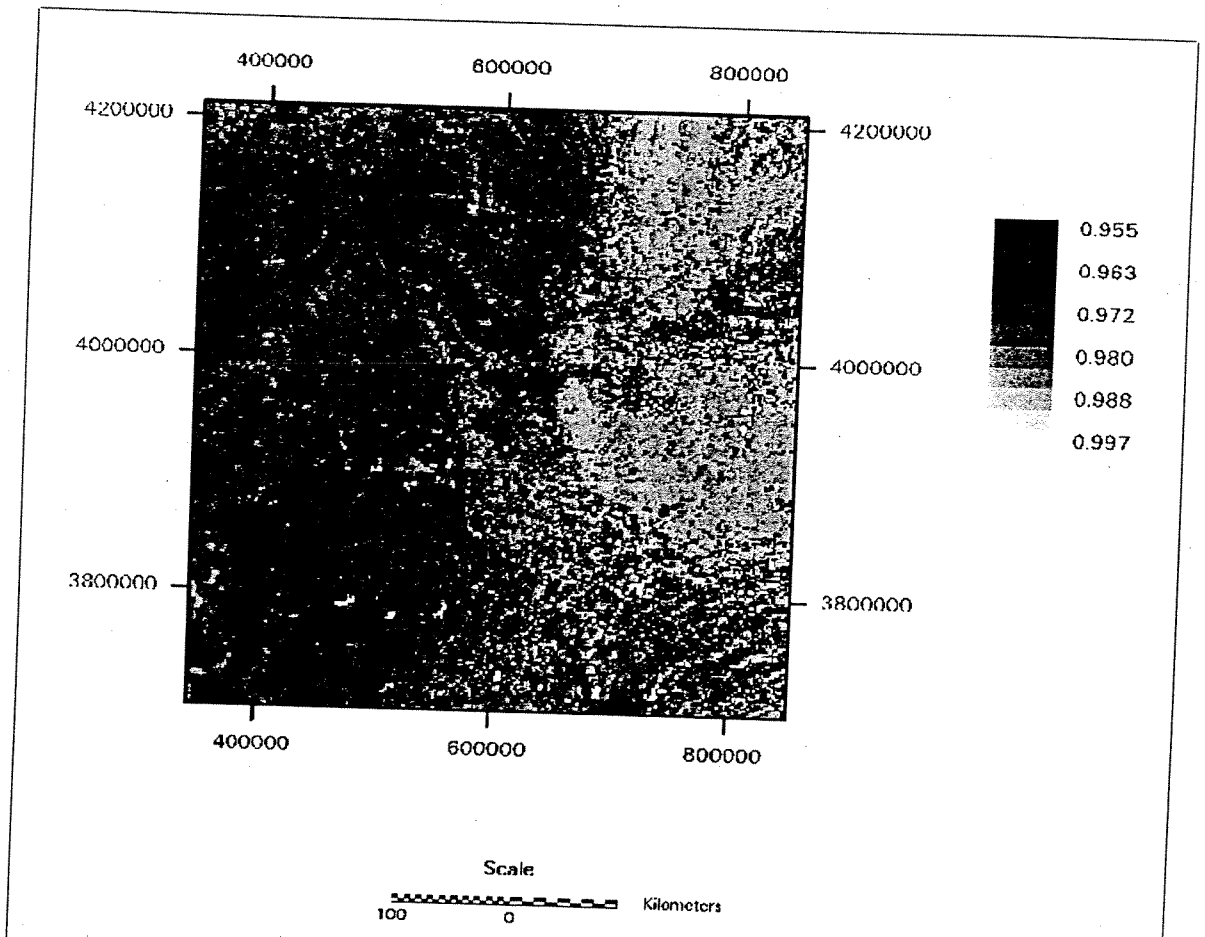

Figure 1. 02 July 1997 emissivity image over the SGP97 study area. Water bodies within the scene are white due to the assigned emissivity value of 0.998.

Figure 2 shows the modeled temperature correction, due solely to changes in emissivity, for nadir. The results are plotted as the at-sensor radiometric temperature of a pixel minus the at-sensor temperature for a perfect emitter. The minimum emissivity was 0.84 and the maximum was 1.0 for the purposes of the model iterations. This range of values encompasses most of the values for natural surfaces reported in the literature. As expected, the role of emissivity becomes larger with an increase in radiometric temperature. For a hypothetical case when the actual emissivity is 0.9 and is treated as 1.0, the magnitude of the temperature correction increases from 4.3°C at an actual radiometric surface temperature of 0°C to 7.3°C at a radiometric temperature of 60°C. These results agree well with those previously reported in the literature (Li and Becker, 1993).

For comparison purposes, the same image was atmospherically corrected without taking emissivity into account (i.e., assuming $\varepsilon = 1.0$). The final radiometric surface temperatures are remarkably different; Figure 3, the histogram of the temperature correction between the two images (emissivity corrected minus not emissivity corrected), demonstrates this. Even though the emissivity range is confined to a small range (0.955 to 0.998), the effect on temperature is apparent. The temperature correction ranged from −1.3°C (corresponding to water pixels) to 8.0°C. The mean temperature change was 3.7°C. The reason for the negative values is due to an additional atmospheric influence, i.e., over land you have a lapse rate with temperature decreasing with height while over water you have an inversion because water generally is much colder than the land. So you have some sort of warmer layer above that is radiating downward. The large peak at about 1.5°C corresponds to the highly vegetated pixels. These values are higher than the theoretical values considered in Figure 2 due to the influence of atmospheric effects in addition to emissivity.

Figure 4 displays the relationship between emissivity and the magnitude of the temperature correction. The triangular shape that is observed is easily explained in terms of physical processes, and are the same reasons as those described in Gillies *et al.* (1997), but the fractional vegetation effects are now viewed through the pixel emissivity values. Thus, the lower emissivities correspond to less vegetated pixels, and have the largest range of temperature correction. This is largely due to variations in soil moisture and topographic influences (i.e., slope and aspect).

One of the primary problems with attempting to take surface emissivity into account when conducting an atmospheric correction is the lack of surface measurements of emissivity. Even if surface measurements do exist, they are not valid at the scale of the AVHRR sensor. If the surface measurements do not exist (as is the case here), one of the best tests for a thermal correction is to compare the vegetated pixels with air temperature observations as the temperature of the air over a dense vegetation canopy should be within a degree or so of the radiometric surface temperature. Therefore, one can validate one's computation within an error of 1 to 2°C. The air temperature measured at a station in the El Reno study area at the time of satellite overpass on 02 July 1997 was 33°C. The full range of temperature over fully vegetated pixels was 27° to 37°C with a mean of

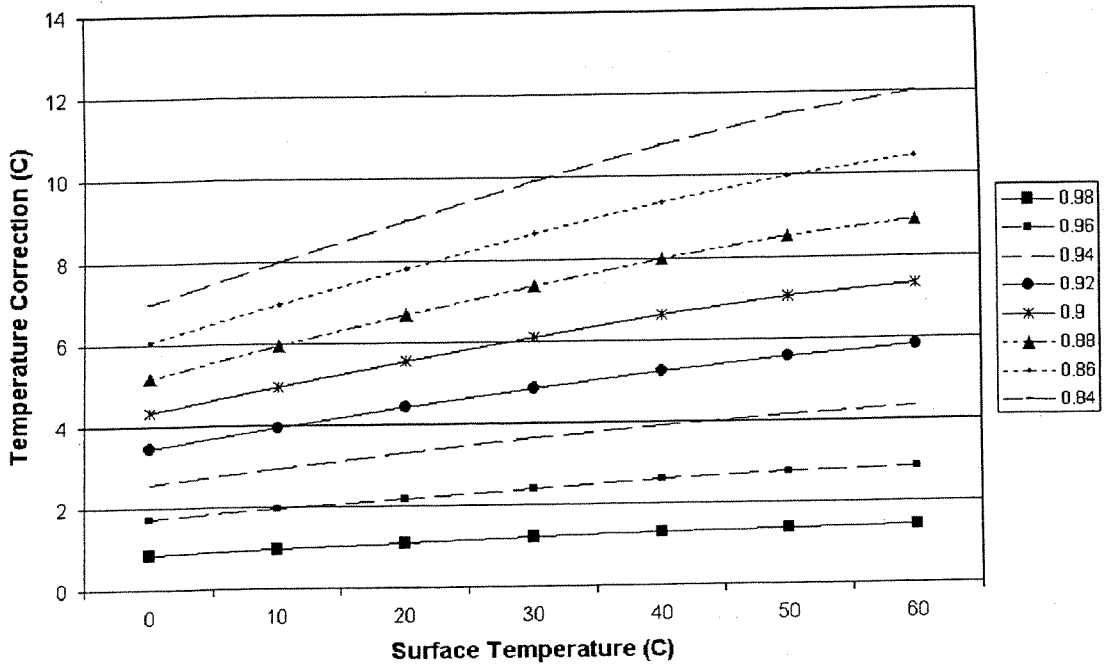

Figure 2. Magnitude of modeled temperature correction as a function of surface radiant temperature and emissivity.

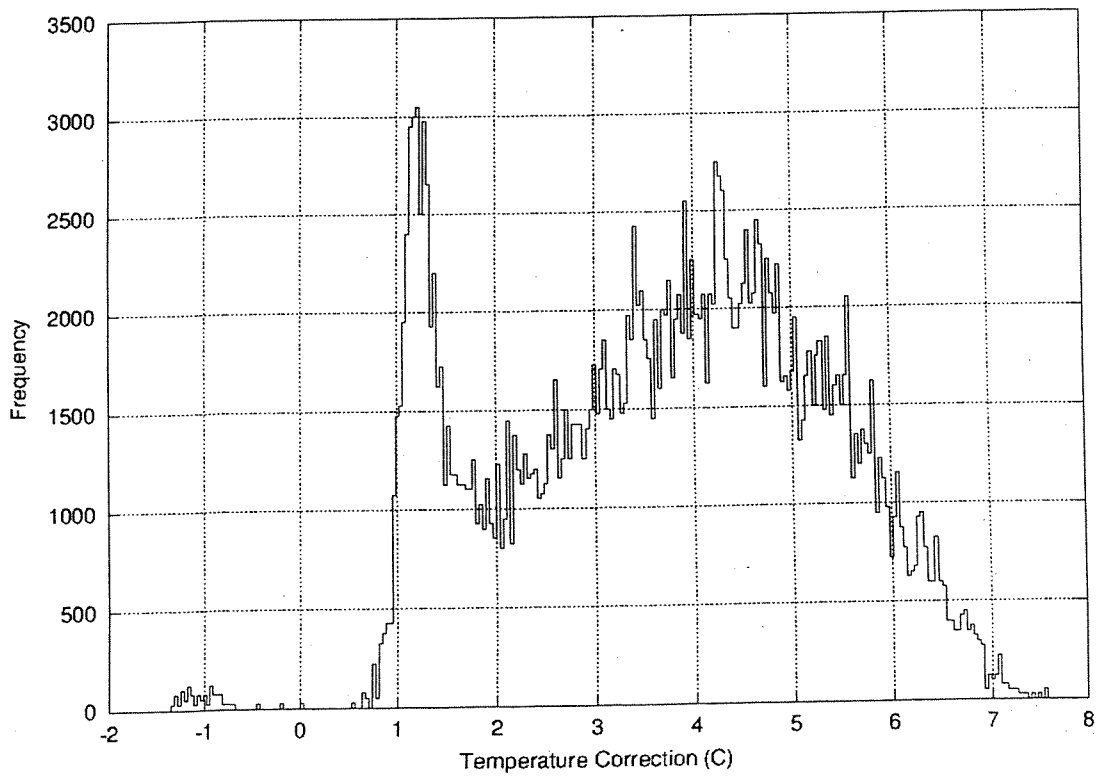

Figure 3. Histogram of magnitude of temperature correction (Corrected minus Non-Corrected). Frequency in this case meaning number of occurrences.

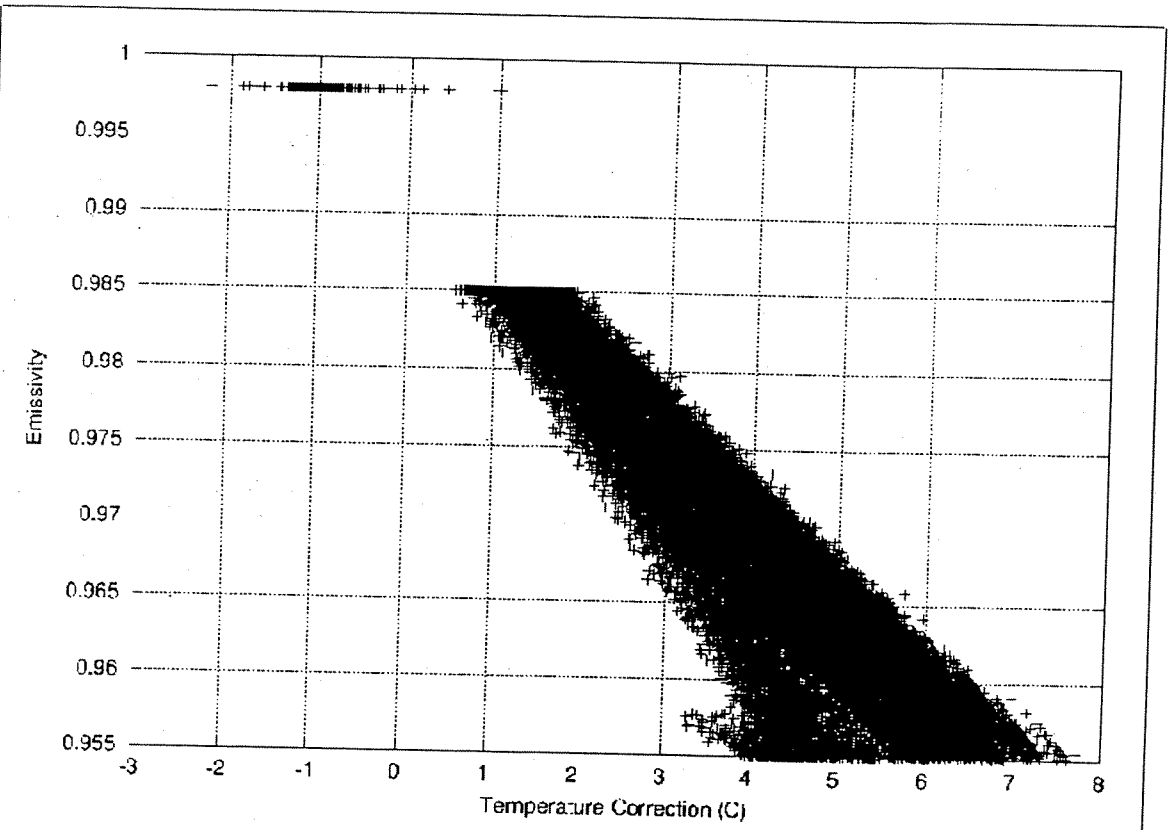

Figure 4. Relationship between the magnitude of observed temperature correction and emissivity. The 0.998 emissivity values represent water covered pixels.

32.5°C. This range of temperatures can be attributed to slope and aspect effects. This is by no means a quantitative validation of the method, but, given the lack of surface measurements, it is a physically sound mechanism for insuring reasonable results. Moreover, the correction for the same conditions over a hot land surface can be significantly higher, and one cannot say whether the error one finds over the vegetation canopy would be indicative of the error over bare dry soil because the errors and the correction both increase with increasing surface temperature.

A comparison with a split window method was not conducted, because it would be impossible to ascribe any differences observed to errors in either method. Without valid surface measurements of radiometric temperature and emissivity at a pixel scale, where these measurements are valid, there can be no validation of this method. Collection of this validation dataset and conducting a validation of the proposed method will be the focus of future research.

Conclusions

It is acknowledged that emissivity is an important consideration in determining radiometric surface temperatures from remotely sensed data, whereupon geophysical variables (such as surface fluxes) which are derived from this temperature are subsequently affected. Its importance is matched by the difficulty of its incorporation. This paper outlines a methodology that offers a relatively straightforward approach for dealing with unknown emissivity values. The benefit of this method over others is the incorporation of the results of Gillies *et al.* (1997) which relates fractional vegetation to N^{*2}, as well as including the influence of emissivity into the atmospheric correction. The method presented in this paper also reiterates the importance of incorporating emissivity when dealing with thermal remotely sensed data.

The methodology was applied to an image over the SGP97 study area taken on 02 July 1997. The mean temperature correction was 3.7°C. There was good agreement between the air temperature and the corrected radiometric temperatures of pixels identified as fully vegetated. Temperature differences of this order can have profound effects when attempting to determine any temperature dependent surface processes. Therefore, it is necessary to account for these changes. The method outlined here is a straightforward way of correcting satellite data for the atmospheric and surface emissivity effects.

Acknowledgments

This study was funded through a grant from NASA Cooperative Agreement No. NCC8-162 in support of the Global Energy and Water Cycle Experiment (GEWEX) Continental Scale International Project (GCIP) and the Utah Agricultural Experiment Station, Utah State University, Logan, Utah.

References

Brunsell, N.A., and R.R. Gillies, 2001. The effect of emissivity on evaporation, *Proceedings, Remote Sensing and Hydrology 2000* (M. Owe, J. Ritchie, and A. Rango, editors), 02–07 April 2000, Santa Fe, New Mexico (International Association of Hydrological Sciences; available at http://www.cig.ensmp.fr/~iahs/) 267:276–280.

Caselles, V., C. Coll, and E. Valor, 1997. Land surface emissivity and temperature determination in the whole HAPEX-Sahel area from AVHRR data, *International Journal of Remote Sensing*, 18:1009–1027.

French, A.N., T.J. Schmugge, and W.P. Kustas, 2000. Estimating surface fluxes over the SGP site with remotely sensed data, *Physics and Chemistry of the Earth (B)*, 25:167–172.

Gillies, R.R., and T. Carlson, 1995. Thermal remote sensing of surface soil water content with partial vegetation cover for incorporation into climate models, *Journal of Applied Meteorology*, 34:745–756.

Gillies, R.R., T. Carlson, J. Cui, W. Kustas, and K. Humes, 1997. A verification of the 'triangle' method for obtaining surface soil water content and energy fluxes from remote measurements of the normalized difference vegetation index (NDVI) and surface radiant temperature, *International Journal of Remote Sensing*, 18:3145–3166.

Kant, Y., and K.V.S. Badarinath, 2000. Studies on land surface temperature over heterogeneous areas using AVHRR data, *International Journal of Remote Sensing*, 21:1749–1756

Kidwell, K.B. (editor), 1998. *NOAA Polar Orbiter Data Users Guide*, National Climatic Data Center, available at http://www2.ncdc.noaa.gov/docs/podug, date last accessed 01 August 2002.

Kniezys, F.X., L.W. Abreu, G.P. Anderson, J.H. Chetwynd, E.P. Shettle, A. Berk, L.S. Bernstein, D.C. Robertson, P. Acharya, L.S. Rotman, J.E.A. Selby, W.O. Gallery, and S.A. Clough, 1996. *The Modtran 2/3 Report and Lowtran 7 Model*, Phillips Lab, Geophysics Directorate, PL/GPOS, Hanscom Air Force Base, Massachusetts, 137 p.

Li, Z.-L., and F. Becker, 1993. Feasibility of land surface temperature and emissivity determination from AVHRR data, *Remote Sensing of Environment*, 43:67–85.

McMillan, L.M., 1975. Estimation of sea surface temperature from two infrared window measurements with different absorptions, *Journal of Geophysical Research*, 80:5113–5117.

Olioso, A., 1995. Simulating the relationship between thermal emissivity and the Normalized Difference Vegetation Index, *International Journal of Remote Sensing*, 16:3211–3216.

Ouaidrari, H., S.N. Goward, K.P. Czajkowski, J.A. Sobrino, and E. Vermote, 2002. Land surface temperature measurement from AVHRR thermal infrared measurements. An assessment for the AVHRR pathfinder II data set, *Remote Sensing of Environment*, 81:114–128.

Qin, Z., and A. Karnieli, 1999. Review article: Progress in the remote sensing of land surface temperature and ground emissivity using NOAA-AVHRR data, *International Journal of Remote Sensing*, 20:2367–2393.

Schott, J.R., 1997. *Remote Sensing: The Image Chain Approach*, Oxford University Press, New York, N.Y., 394 p.

Schmugge, T., S.J. Hook, and C. Coll, 1998. Recovering surface temperature and emissivity from thermal infrared multispectral data, *Remote Sensing of Environment*, 65:121–131.

Sobrino, J., Z-L Li, M.P. Stoll, and F. Becker, 1994. Improvements in the split window technique for land surface temperature determination, *IEEE Transactions on Geoscience and Remote Sensing*, 32:243–253.

Sobrino, J., N. Raissouni, and Z.-L. Li, 2001. A comparative study of land surface emissivity retrieval from NOAA data, *Remote Sensing of Environment*, 75:256–266.

Valor, E., and V. Casselles, 1996. Mapping land surface emissivity from NDVI: Application to European, African, and South American areas, *Remote Sensing of Environment*, 57:167–184.

Van de Griend, A., and M. Owe, 1993. On the relationship between thermal emissivity and the normalized difference vegetation index for natural surfaces, *International Journal of Remote Sensing*, 14:1119–1131.

Walton, F.F., E.P. McClain, and J.F. Sapper. 1990. Recent changes in satellite-based multi-channel sea surface temperature algorithms. MTS90, Marine Technology Society, Washington, D.C.

(Received 10 September 2001; revised and accepted 08 May 2002)